Journal of Hazardous Materials, 16 (1987) 185-199
Elsevier Science Publishers B.V., Amsterdam — Printed in The Netherlands

TRANSLATIONAL CLOUD SPEEDS IN THE THORNEY ISLAND TRIALS: MATHEMATICAL MODELLING AND DATA ANALYSIS

C.J. WHEATLEY* and A.J. PRINCE

Safety and Reliability Directorate, United Kingdom Atomic Energy Authority, Wigshaw Lane, Culcheth, Warrington, WA3 4NE (Great Britain)

(Received October 16, 1986; accepted March 3, 1987)

Summary

The speed of a toxic or flammable heavy gas cloud is important for determining its hazardous effect. An equation of motion for translation of the cloud as a whole is derived and suggestions are made for parameterisation of the terms in the equation. These are tested by comparison with the photographic and concentration data from the Phase I trials. The data show that the ratio of the cloud and wind speeds rapidly tends to a constant value early on, but later settles down to a value which depends on the cloud Richardson number. The comparison suggests that the early motion is dominated by momentum bought into the cloud by entrainment, while the later motion results from a balance between shear stresses at the top of the cloud and the ground.

1. Introduction

The translational motion of a toxic or flammable heavy gas cloud is important to the hazard posed both in respect of the distance travelled and the time of passage. Its importance was emphasized by the analysis of the Thorney Island Phase I data by Wheatley et al [1,2]. Using the area-averaged concentrations obtained by Brighton [3,4] it was shown that a simple box model can provide a consistent fit to the data when the usual entrainment model is used with edge entrainment coefficient equal to 0.7 and with top entrainment velocity modelled in the following way:

$$U_{\mathrm{T}} = U_{\mathrm{c}}/Ri \tag{1}$$

$$Ri = g\Delta\rho h/\rho_{\mathrm{a}} U_{\mathrm{c}}^2 \tag{2}$$

U_{c} is the speed of the cloud centroid, for which measured values were used, Ri is the Richardson number based on U_{c}, g is acceleration due to gravity, $\Delta\rho$ is equal to $\rho-\rho_{\mathrm{a}}$ where ρ is the density of the cloud, ρ_{a} is the density of air and h

*Present address: UKAEA Attaché, Sandia National Laboratories, Division 6425, P.O. Box 5800, Albuquerque, NM 87185, U.S.A.

0304-3894/87/$03.50

is the height of the cloud. Using U_c as the velocity scale in U_T provided an explanation for the observation that clouds diluted less rapidly with respect to time the slower they travelled. U_c is consequently also important for the rate of dilution of the cloud.

The cloud speed is usually taken by modellers to be either the wind speed at 10 m or the wind speed at some constant fraction of the cloud height. It was shown by Wheatley et al. that these models are not consistent with the data. The cloud speed at later times was found to be strongly dependent on the initial Richardson number based on the wind speed at 10 m, Ri_0. In contrast, an examination of the results obtained from the photographic data by Brighton et al. [5] (see also Ref. [6]) shows this behaviour not to be present at early times.

Some understanding of the translational motion of a heavy gas cloud is therefore required. We therefore ask: What does the Thorney Island data imply for modelling the cloud speed?

To answer this question we first obtain the general form for an equation of motion and then consider how each term might be parameterised for a heavy gas in the box model framework. Certain constants are estimated by the requirement that the correct speed should be obtianed in the passive limit.

Some aspects of the equation are uncertain or unknown and prevent immediate integration of the full equation. Our strategy is therefore to use the equation to guide our analysis of the data with a view to confirming or otherwise the suggested parameterisations and to fix remaining unknowns. The photographic data is uded to study the behaviour at early times and the concentration data is used to study the behaviour at later times. We conclude by offering a tentative physical interpretation of the observations and discussing the possible wider validity of the equation of motion.

2. The equation of motion

2.1 The integrated momentum equation

Momentum can be transferred to a heavy gas cloud in a number of ways. To see this it is convenient to start from the ensemble averaged momentum equation expressed as a differential equation

$$\frac{\partial}{\partial t}(\rho U_i) = -\frac{\partial}{\partial x_k}\Pi_{ik} - \rho g \delta_{i3} \tag{3}$$

U_i is the i-th component of the mean flow velocity, g is acceleration due to gravity and Π_{ik} is the tensor given by

$$\Pi_{ik} = p\delta_{ik} + \rho U_i U_k + \rho\overline{u_i' u_k'} \tag{4}$$

where p is the mean pressure and $\overline{u_i' u_k'}$ is the Reynolds stress tensor. The viscous stress term has not been included in eqn. (4) because it is negligible in the present case.

Equation (3) is now integrated over a volume V bounded by a surface S, where V and hence S are allowed to vary with time, to obtain

$$\overset{\text{I}}{\frac{\mathrm{d}}{\mathrm{d}t}\left(\int_V \rho U_i \mathrm{d}V\right)} = \overset{\text{II}}{-\int_S p\,\mathrm{d}S_i} \overset{\text{III}}{-\int_S \rho\,\overline{u_i' u_k'}\mathrm{d}S_k} \overset{\text{IV}}{-\int_S \rho\,U_i U_k\,\mathrm{d}S_k}$$

$$\overset{\text{V}}{+\int_S \rho U_i U_k^{\mathrm{s}}\,\mathrm{d}S_k} \overset{\text{VI}}{-\int_V \rho g \delta_{i3} \mathrm{d}V} \quad (5)$$

The terms have been labelled I to VI for convenience. Term V arises from taking the time derivative outside the integral in Term I, where U_k^{s} is the k-th component of the velocity of the surface S. Term V with Term IV is the net rate at which momentum is transported into V by fluid crossing its boundaries. The interpretation of the terms for a heavy gas cloud is discussed in the next sub-section.

2.2 Application to a heavy gas cloud

Equation (5) projected on the wind direction forms the basis of an integral equation of motion for a heavy gas cloud. The cloud is assumed to be just within the region V which is taken to be a right cylinder of radius R and height h and with constant (i.e., volume-averaged) properties inside. Suggested parameterisations of the terms are as follows:

$$\text{Term I} \quad = \quad \frac{\mathrm{d}}{\mathrm{d}t}(\rho V U_{\mathrm{c}}) \quad (6)$$

This is the rate of change of momentum within V. The volume V now equals $\pi R^2 h$.

$$\text{Term II} \quad = \quad 0 \quad (7)$$

This is the form drag term whose neglect can be justified providing Ri_0 is large enough.

$$\text{Term III} \quad = \quad A(\tau_{\mathrm{T}} + \tau_{\mathrm{G}}) \quad (8)$$

where τ_{T} and τ_{G} are the turbulent shear stresses at the top of the cloud and the ground, respectively. A equals πR^2. A term due to turbulent shear stresses at the cloud edges is of similar magnitude to Term II and is neglected. Parameterisations for τ_{T} and τ_{g} are discussed in the next sub-section.

$$\text{Terms IV and V} = \rho_a \frac{dV}{dt} \beta U_w \quad (9)$$

This stands for momemtum brought into the cloud by entrainment. dV/dt is the rate of volume increase, U_w is the wind speed evaluated at the cloud top and β is a constant factor to account for non-uniformity of the flow field over S. We shall later consider an alternative parameterisation in which the factor βU_w is replaced by $\frac{1}{2}(\beta U_w + U_c)$.

Bradley et al. [7] have suggested that the contributions to dV/dt in eqn. (9) arising from edge and top entrainment should be treated separately. This is discussed in more detail later.

$$\text{Term VI} = 0 \quad (10)$$

This is zero because the cloud motion is assumed to be horizontal.

The equation of motion for a heavy gas cloud is therefore taken as

$$\frac{d}{dt}(\rho V U_c) = \rho_a \frac{dV}{dt} \beta U_w + A(\tau_T + \tau_G) \quad (11)$$

Although the above equation might have been written down straight away on intuitive grounds, we have preferred to start from eqn. (3) to illucidate two aspects which are not, in our view, obvious. The first concerns whether we have "double counted" the momentum brought into the cloud by entrainment by including terms propotional to dV/dt on both the left and right hand side. The derivation shows this is not the case. The second concerns the velocity scale in the first term on the right hand side. The derivation makes clear there is some flexibility in its choice, which we later investigate.

2.3 The shear stress terms

The shear stress at the ground is straightforwardly modelled as

$$\tau_G = -\tfrac{1}{2} C_f \rho_a U_c^2 \quad (12)$$

C_f is a friction factor which we estimate from the ambient wind profile by equating the usual expression for the shear stress at the ground, $\rho_a u_*^2$, with an estimate analogous to eqn. (12), giving

$$\tfrac{1}{2} C_f = u_*^2 / U_w^2(\eta' h/2) \quad (13)$$

where u_* is the friction velocity and η' is a constant to be found. The factor $\frac{1}{2}$ is included in the argument of U_w for later convenience ($h/2$ is the height of the cloud centroid in the box model framework).

The shear stress at the cloud top is expected to depend on the velocity difference $U_w(h) - U_c$ and on the stratification by way of a Richardson number Ri. We therefore assume, essentially on dimensional grounds, that

$$\tau_T = \rho_a (U_w(h) - U_c)^2 f(Ri) \quad (14)$$

where f is a presently unknown function of Ri.

It is convenient here to consider the passive limit of a heavy gas cloud since this enables estimates for U_c/U_w in the passive limit and C_f to be obtained for later use.

It is assumed that eventually the cloud speed is determined by a balance of shear stresses at the top of the cloud and the ground

$$\tau_T = -\tau_G \tag{15}$$

and we require this to lead to the correct speed of travel of the cloud in the passive limit.

The balance of shear stresses leads to

$$\tilde{U}_c^2/(1-\tilde{U}_c)^2 = 2f(Ri)/C_f \tag{16}$$

where $\tilde{U}_c = U_c/U_w(h)$.

In the passive limit $Ri \to 0$ and we expect

$$f(Ri) \to \gamma \tag{17}$$

where γ is a constant.

The cloud speed in this limit is given by

$$\tilde{U}_c = 1/\{1+(C_f/2\gamma)^{\frac{1}{2}}\} \tag{18}$$

γ and η' are estimated by comparing this with the theoretical result of Chatwin [8] for passive dispersion of a puff in an adiabatic boundary layer* given by

$$\tilde{U}_c = \log_e(\eta h/2z_0)/\log_e(h/z_0) \tag{19}$$

where η is 0.561.... and z_0 is the roughness length. Using the logarithmic wind profile in eqn. (13) to estimate C_f and eqns. (18) and (19) one finds

$$\log_e(\eta h/2z_0) + \frac{\kappa \log_e(\eta h/2z_0)}{\gamma^{\frac{1}{2}} \log_e(\eta' h/2z_0)} = \log_e(h/z_0) \tag{20}$$

where κ is the von Karman constant. If η' is chosen to equal η then eqn. (20) becomes independent of h and z_0, and the following equation is found for γ

$$\gamma = \kappa^2/\log_e^2(2/\eta) \approx 0.1 \tag{21}$$

Substituting the values found for η' and γ into eqns. (13) and (18) with z_0 equal to 6×10^{-3} m and h equal to 2–4 m (values typical of the Thorney Island trials) leads to $\tilde{U}_c$ in the passive limit ≈ 0.8 and $C_f \approx 0.01$.

*The boundary layers during the Thorney Island trials were not adiabatic. However, we do not expect $\tilde{U}_c$ in the passive limit and C_f to be strongly dependent on the Monin–Obukhov length.

3. Comparison with the data

3.1 Behaviour at early times

Overhead and sideview photographs were taken at frequent intervals during the trials. These photographs enable the motion of the cloud to be studied over the early period of each trial when the cloud outline is sufficiently well defined. Brighton et al. [5] have analysed the Phase I overhead photographs to obtain estimates for the area, denoted A_t, and the distance of centroid from the release point, denoted X_t, and Beesley [9,10] has analysed the Phase I sideview photographs to obtain estimates for area, denoted A_s, and height, denoted h_s, as functions of time over these periods. These results are used here.

First we return to the equation of motion to obtain guidance on how to further process the results. We assume that τ_T and τ_G can be neglected. (This is justified later, after an estimate has been obtained for τ_T.) Taking U_w to be constant*, the simplified equation of motion can now be integrated to give

$$\tilde{U}_c = \beta\{1-\rho_0 V_0/\rho V\} = \beta\{1-(1+\Delta_0')/(\tilde{V}+\Delta_0')\} \tag{22}$$

using the fact that buoyancy is conserved. Δ_0' is the initial density difference of the cloud relative to air and $\tilde{V}$ equals V/V_0 where V_0 is the initial volume of the cloud. This equation suggests that $\tilde{U}_c$ and $\tilde{V}$ should be found from the data and the dependence of $\tilde{U}_c$ on $\tilde{V}$ studied.

The cloud speed can be obtained from X_t. Random noise in the data results in erratic values for U_c if estimated by differencing successive values of X_t. Instead X is expressed as a sum of Chebyshev polynomials and U_c is obtained from dX/dt. The coefficients in the expansion were found by minimising

$$\epsilon_n^2 = \sum_{t_i} [X(t_i) - X_t(t_i)]^2 / A_t(t_i) \tag{23}$$

where t_i denotes the successive times at which estimates are available for X_t and A_t. The weighting $1/A_t$ is included on the assumption that the error in locating the position of the cloud centroid is proportional to $A_t^{\frac{1}{2}}$. The subscript n denotes the maximum order of polynomial included in the expansion. This was chosen by studying the bahaviour of ϵ_n as a function of n. Good separation in wavelength between the random noise and systematic behaviour was found. n equals 3 was found to provide an adequate fit to the systematic behaviour for all trials studied.

U_w was obtained from the wind speeds measured at the meteorological mast by the cup anemometers at 2 m and 10 m. They were averaged over three minutes centred at the time of the release. U_w was then found by interpolating between these two measured wind speeds using a power law profile. The height at which the interpolation was done was taken to be the time average of h_s, ignoring the rapid descent of the cloud immediately after release.

---

*U_w in fact varies with h but only by a small amount over the ranges of h we consider in our comparison and can be neglected.

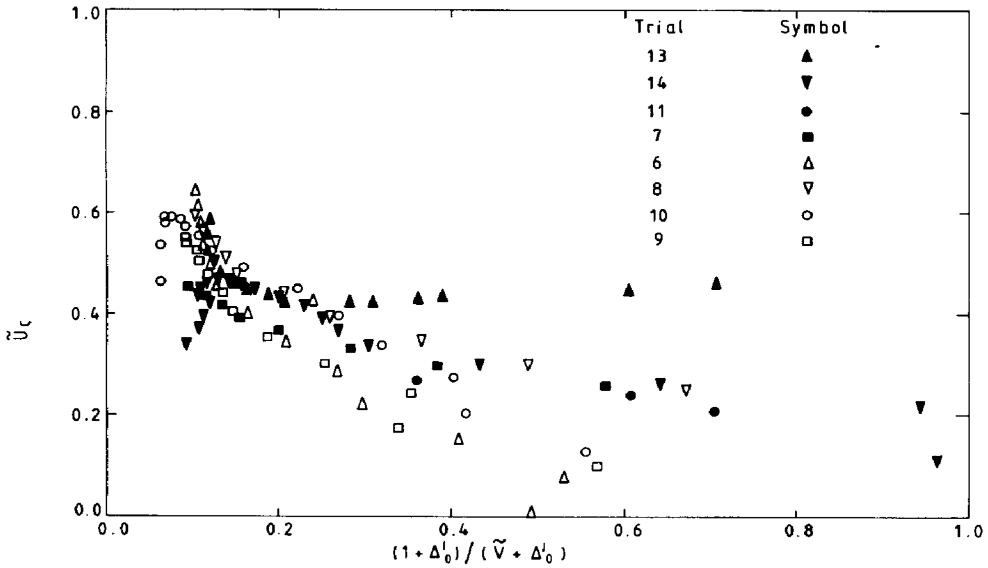

Fig. 1. Plot of non-dimensionalized cloud speed against the function shown of the cloud volume where the volume has been estimated from the cloud area and height. The trials are listed in order of increasing initial Richarson number.

V in principle could be estimated as $A_t h_s$ ($A_s h_s$ is not used since A_s overestimates the cloud area — see below), but, the overhead and sideview cameras were not synchronised and the discrepancy was not recorded. Fortunately this can be estimated by comparing A_t with A_s. A_s is generally larger than A_t due to a line-of-sight effect of the sideview analysis [9,10]. This effect is small when the cloud area is small and during this time the estimates A_t and A_s should be similar in size. The amount of asynchronisation was hence estimated by shifting the time axis of A_s to achieve the best agreement between A_t and A_s early on. The height to be combined with A_t to estimate V was then found as a linear interpolation of the two values of h_s either side in time of A_t. (For most trials two sets of estimates for h_s were available from cameras at two positions on the ground. The interpolation was done for each set separately and the results then averaged.) A check on the estimated asynchronisation was provided by studying the resulting estimate for V which should increase smoothly with time. This was found to be so in all cases.

Figure 1 shows $\tilde{U}_c$ plotted against $(1+\Delta'_0)/(\tilde{V}+\Delta'_0)$ for Trials 6–11, 13 and 14. The trials are listed in the figure in order of increasing Ri_0. There is no clear evidence of a dependence of $\tilde{U}_c$ on Ri_0. This suggests that Ri_0 is sufficiently large to justify neglect of form drag and shear stress at the cloud edge in all trials.

Equation (22) implies that the data should lie on a straight line passing

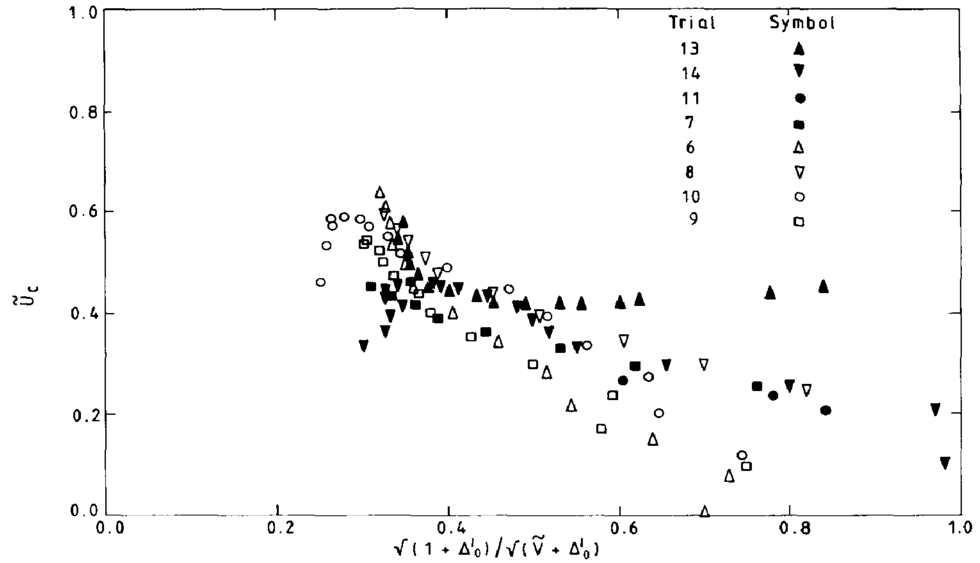

Fig. 2. Plot of non-dimensionalized cloud speed against the function shown of the cloud volume where the volume has been estimated from the cloud area and height. The trials are listed in order of increasing initial Richardson number.

through the point (1,0). The data show a fairly consistent trend of increasing $\tilde{U}_c$ with increasing $\tilde{V}$ but not on a straight line. The errors in $\tilde{U}_c$ are small enough at larger dilutions for this to be a significant deviation.

One possible explanation lies in the use of h_s to estimate V. h_s is in general an overestimate of the area-averaged height of the cloud; the cloud edges might be expected to be somewhat higher than the cloud height towards the centre. $\tilde{V}$ might therefore be over-estimated. To test this, $\tilde{V}$ was instead estimated from $(A/A_0)^{0.7}$ where A_0 is the initial cloud area, using the findings of Wheatley et al. [1, 2, 11]. The deviation from a straight line was found to remain.

We therefore conclude that the suggested parameterisation for Terms IV and V in eqn. (5) is incorrect. The integration leading to eqn. (9) was done assuming the ambient flow field was little affected by the presence of the cloud. The average flow speed in the integration was therefore taken as βU_w. It is possibly more appropriate to take instead $(\beta U_w + U_c)/2$, i.e. the mean of that for the ambient flow field and that for the cloud. Terms IV and V become $\rho_a(dV/dt) \times (\beta U_w + U_c)/2$ and the modified equation of motion appropriate to the early motion leads to

$$\tilde{U}_c = \beta\{1 - \surd(1+\Delta_0')/\surd(\tilde{V}+\Delta_0')\} \tag{24}$$

Figure 2 shows the same data as in Fig. 1, but instead plotted as a function of $\surd(1+\Delta_0')/\surd(\tilde{V}+\Delta_0')$. Equation (24) predicts that the data should lie on a straight line passing through (1,0) and on the whole this appears to be the case. By eye the value of β which gives the best fit to the data is 0.8.

Remembering that β is a factor included to account for non-uniformity of the flow field over the cloud surface, it is of interest to calculate an effective height from which the air comes. Equating $\beta U_w(h)$ to $U_w(h_e)$ we find $h_e \approx 0.35\ h$. It can be shown from the findings of Wheatley et al. [1, 2] that edge entrainment dominates top entrainment over the period for which the analysis has been done in all trials. The value found for h_e is therefore reasonable.

It is necessary to check our assumption that shear stresses at the ground and cloud top could be neglected. Firstly, we have estimated f in τ_T as $1/1000\ Ri$, based on the findings of Sub-section 3.2. Using this we estimate that the shear stress at the ground is larger than the shear stress at the cloud top over the period studied in all trials. Secondly, we find that the effective force associated with entrainment is larger than the force at the ground by generally a factor of ten or more, decreasing to a factor of roughly four for the last few points in some of the trials. We therefore find that shear stresses at the ground and cloud top can be neglected for this analysis.

It is concluded that with the new choice of velocity scale replacing that in eqn. (9) the data in Fig. 2 show that $\tilde{U}_c$ tends to a constant value (β) with increasing $\tilde{V}$ in the early stages of motion. The data shows little dependence on Ri_0. Comparison with the equation of motion shows that this behaviour is apparently due to momentum brought into the cloud by entrainment. The limit is not reached in practice because shear stresses do eventually become important as discussed below.

Behaviour at later times

The behaviour $\tilde{U}_c \rightarrow \beta$ found for the early time behaviour will not hold indefinitely in general because drag with the ground becomes increasingly important as the cloud spreads causing the cloud to slow down until, presumably, a balance between stresses at the top of the cloud and the ground is established. In Brighton [4] and Brighton et al. [5] the concentration data is analysed over a period which starts just before the photographic data used for the analysis in Sub-section 3.1 ends, and extends to when the cloud leaves the sensor array, generally some 700 m from the point of release. Estimates for cloud speeds were obtained in this anaysis. The clouds in all Phase I trials have large aspect ratio over this period and so we expect this data to provide information relevant to a phase of motion different from that studied at early times.

We again return to the equation of motion for guidance on how to analyse the data. We assume that the shear stresses at the top of the cloud and the ground are balanced. This leads to eqn. (16) which suggests that $\tilde{U}_c$ is a function of the Richardson number, Ri, to be defined. The function f of Ri in eqn. (16) is unknown which suggests that a plot of $\tilde{U}_c^2/(1-\tilde{U}_c)^2$ against Ri would be useful. Estimates are therefore required for $\tilde{U}_c$ and Ri.

Translational motion of the cloud was studied in Brighton [4] from an analysis of arrival and departure times at masts with concentration sensors. Estimates were obtianed for the speeds of the centres of curvature of the forward and rearward edges of the cloud, U_f and U_r respectively, as the slope of a straight line fit to the positions of the centres of curvature, X_f and X_r, plotted against time. U_c is estimated from these results as

$$U_c = (U_f + U_r)/2 \tag{25}$$

This estimate is assumed to be valid for a time period t_- to t_+ over which the straight line behaviour for both X_f and X_r is judged to be valid.

Ri and other properties of the cloud change by substantial amounts over the time period t_- to t_+. Other quantities required for the analysis are therefore evaluated at t_-, t_0 and t_+, where t_0 is the arithmetic mean of t_- and t_+.

U_w is obtained similarly to that described earlier. Three minute time averages of the measured wind speeds centred at t_-, t_0 and t_+ are used. The cloud height is required for the interpolation. It is estimated by assuming a uniform vertical concentration profile and conservation of mass leading to

$$h = h_0 C_0 / \tilde{A} C(t) \tag{26}$$

where h_0 and C_0 are the initial height and concentration respectively, $C(t)$ is the area average concentration found by Brighton [3] and $\tilde{A}$ is defined by

$$\tilde{A} = A/A_0 \tag{27}$$

$\tilde{A}$ is estimated from

$$\tilde{A} \approx (t - \Delta t)/T_0 \tag{28}$$

where t is the elapsed time from release. T_0 is the buoyancy time scale and Δt is a small time shift both taken from Brighton et al. [5]. It was shown there that eqn. (28) leads to estimates for $\tilde{A}$ within a factor 2 — this is adequate for our purpose.

Ri is a measure of the importance of stratification between the cloud and the ambient flow field for preventing transfer of momentum to the cloud by shear stresses. An appropriate definition is

$$Ri = g \Delta\rho h / \rho_a U^2 \tag{29}$$

where U is an as yet unspecified velocity scale. Buoyancy conservation enables Ri to be rewritten as

$$Ri = g \Delta_0' h_0 / \tilde{A} U^2 \tag{30}$$

The question remains what velocity should be chosen for U. The analysis of Wheatley et al. [1, 2] showed that the velocity scale in the analogous Richardson number for transfer of mass should be taken as U_c in order to fit the concentration data. It was suggested that U_c was a measure of the velocity scale of turbulence within the cloud opposing the effect of the stratification. It is suggested that U_c is a reasonable choice for U also.

Figure 3 shows $\tilde{U}_c^2/(1-\tilde{U}_c)^2$ plotted against Ri for Trials 5–9 and 11–19. The central point for each trial is evaluated at t_0 and the outer points are evaluated at t_- and t_+. The figure reveals a clear correlation between $\tilde{U}_c$ and Ri. A straight line fit by eye leads to

$$f=10^{-3}/Ri \tag{31}$$

The passive limit for $\tilde{U}_c$ is indicated on the figure. From this it seems that the translational motion of all trials except possibly Trials 15 and 18 was affected by density stratification over the whole period t_- to t_+ for each trial.

Substituting eqn. (31) in eqn. (16) and writing Ri in terms of Ri_w, where Ri_w is the Richardson number based on wind speed, one finds $\tilde{U}_c=0$ for finite Ri_w. We would not attach much weight to this extrapolation since one finds Ri_w must be infinite to obtain $\tilde{U}_c=0$ for $f \propto Ri^{-\alpha}$ with $\alpha<1$. The data do not rule out this alternative for f.

An alternative choice for U in Ri is U_w. If $\tilde{U}_c$ and Ri are related then it is irrelevant whether Ri is based on U_c or U_w, but it may affect the simplicity of the relation. Figure 4 shows $\tilde{U}_c^2/(1-\tilde{U}_c)^2$ plotted against Ri based on the wind speed. From this it can be seen that there is no clear advantage to be gained from this alternative. The correlation given by eqn. (31) is also shown in the figure.

With an estimate for f, we can check our assumption that shear stresses at the cloud top and ground are balanced. The left hand side of eqn. (11) leads to a term proportional to $\mathrm{d}U_c/\mathrm{d}t$. U_c was estimated for a period in each trial over which a straight line fit of X_r and X_f to t was judged reasonable, i.e. $\mathrm{d}U_c/\mathrm{d}t \approx 0$ and so we assume that it is reasonable to ignore this term. The remaining terms in eqn. (11) we have neglected are proportional to $\mathrm{d}V/\mathrm{d}t$. We use the results of Wheatley et al. [1, 2] to estimate $\mathrm{d}V/\mathrm{d}t$ and compare these terms with $A\tau_T$. With $\beta=0.8$ we find they are less than $A\tau_T$ by generally a factor of three. This is not so always. In those trials for which edge entrainment dominates, primarily at t_- in about half the trials, we find the effective force associated with the $\mathrm{d}V/\mathrm{d}t$ terms is comparable to our estimate for $A\tau_T$. Leaving aside these data points, for which information about shear stress at the cloud top will be very uncertain, we can revise our estimate for f by accounting for the contributions of the terms involving $\mathrm{d}V/\mathrm{d}t$. We find that our estimate remains consistent with the data but with increased scatter of the points. It was assumed $\beta=0.8$ in the analysis above. However, it was shown earlier that this estimate is valid for edge entrainment. We might expect $\beta>0.8$ for top entrainment, but we find the scatter on the data is too large to enable estimates for β and f to be simultaneously extracted. There seems to be no alternative to choosing $\beta=0.8$ for top entrainment also.

It is conclude that the data at later times show that the cloud speed when

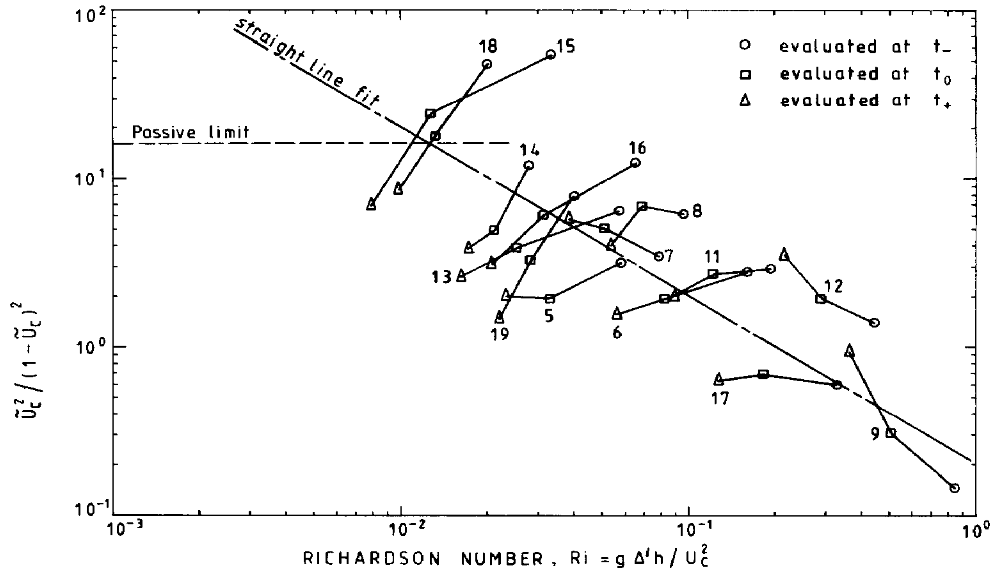

Fig. 3. Correlation between a function of the cloud speed and the Richardson number based on the cloud speed. The numbers adjacent to the points denote the trial numbers.

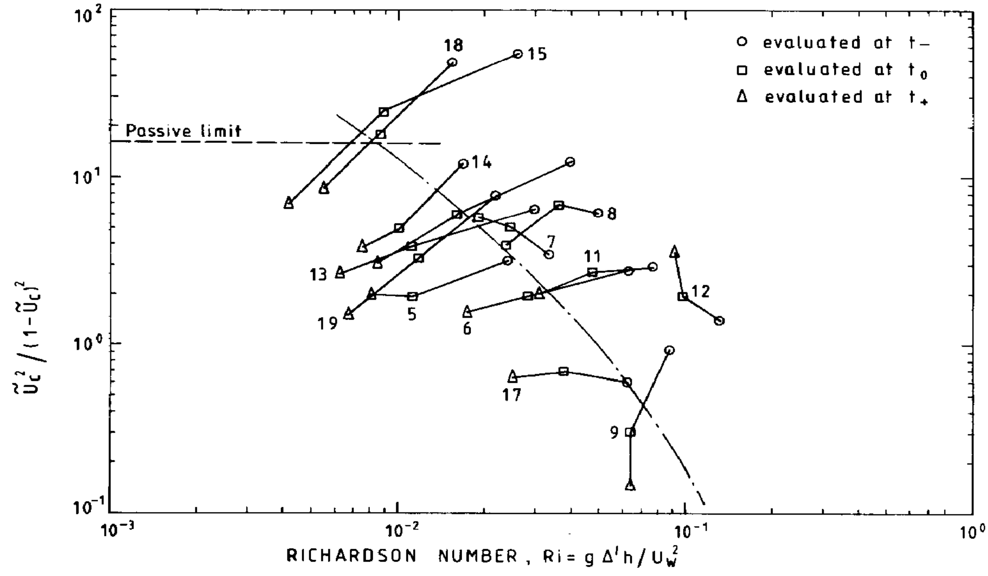

Fig. 4. Correlation between a function of the cloud speed and the Richardon number based on the wind speed at the cloud top. The numbers adjacent to the points denote the trial number.

non-dimensionalised with the wind speed at the cloud top is correlated with the layer Richardson number, Ri. Comparison with the equation of motion suggests that this behaviour is due to a balance between shear stresses at the cloud top and the ground. An estimate for the functional dependence of the shear stress at the cloud top on the Richardson number has been obtained from the data. This interpretation provides an explanation for the observed slow speeds of travel (in terms of $\tilde{U}_c$) seen in Trials 9, 12 and 17, these being the trials with largest initial Richardson number for which the effects of stratification on the translational motion are greatest. This in turn leads to lessened dilution rates [1, 2].

3.3 Discussion

We consider to what extent the correlations found in the data are reliable and the suggested equation of motion may be more generally applicable.

A number of uncertainties originate from experimental error. Figures 1 and 2 for the early time analysis show considerable variation in $\tilde{U}_c$ from trial to trial when $\tilde{V}$ is small. However, the variation is believed to be largely due to error in the data. First, the error in the estimated cloud speed is largest when the slope of the curve fitted to X changes most rapidly (since fewer points determine the slope in these regions): second, the error in X is increased when the cloud obscures the release point; and third, the error in $\tilde{V}$ due to asynchronisation between h_s and A_t is largest when h changes most rapidly. These three errors are all prominent when $\tilde{V}$ is small. The scatter unfortunately masks any dependence of U_c on Ri_0 which may be present in the data. At larger $\tilde{V}$ the errors are less and it can be seen from the figures that the variation here is also less.

For the later time behaviour, the bars in Figs. 3 and 4 are not error bars but originate from using an average of the cloud speed in each trial over a period for which Ri changes considerably (by as much as a factor of five). The estimation of Ri is in itself subject to error, mainly through approximating $\tilde{A}$ by $(t-\Delta t)/T_0$. Error is also present in U_c which is amplified in the function $\tilde{U}_c^2/(1-\tilde{U}_c)^2$ plotted on the ordinate. These lead to considerable scatter in the figure. This is counterbalanced by the data spanning two and nearly two orders of magnitude in the ordinate and abscissa respectively; on this scale, the scatter is relatively small.

The motion being studied is complex. It was seen in both the early and later behaviour that there is considerable freedom in choosing parameterisations for the entrainment and shear stress terms. This freedom derives from the multiplicity of possibly relevant velocity and length scales. Although the data span a large range of Ri_0, this range stems essentially from variation in the wind speed. Other scaling parameters, such as h_0/R_0, h_0/z_0 and Δ_0', changed very little if at all from trial to trial. Varying these parameters may reveal effects not encompassed by the suggested parameterisations. This is also important to the question of the wider applicability of the suggested equation of motion. Certain terms were neglected in deriving this equation, for example, form drag and shear stress at the cloud edge. These could be important for releases with small Ri_0.

In the light of this discussion we suggest that independent confirmation of the correlations is desirable. For example wind tunnel experiments might be done or studies made of the component phenomena. It would also be of interest to study the translational motion of a continuous heavy gas release for which the flow field above the cloud might be expected to be modified by the presence of the cloud to a greater extent than for an instantaneous release. Such trials were performed later in the Thorney Island trials series. It remains to be seen whether they show a measurable difference in translational motion when compared with the instantaneous trials.

It is concluded that one must be cautious in accepting that the correlations have been confirmed by the data or can be extrapolated by applying the equation of motion to other cases. On the other hand the quality of the correlations is good by the standards of field trials in general and we believe they reflect a real systematic behaviour in the trials.

4. Conclusions

An integral equation of motion for the translational motion of a heavy gas cloud as a whole has been derived and suggestions have been made for parameterisations of the terms in the equation. These have been tested by comparison with the photographic and concentration data from the Phase I trials.

Analysis of the data at early times has shown that the ratio of the cloud speed to the wind speed tends to a constant value of about 0.8. Comparison with the equation of motion shows that the early motion is apparently due to momentum brought into the cloud by entrainment. The limit, however, is not actually reached before shear stresses become important.

Analysis of the data at later times has shown that the ratio of the cloud speed to the wind speed depends on the cloud Richardson number. Comparison with the equation of motion shows that this is apparently due to a balance between shear stresses at the cloud top and the ground. The functional dependence of the shear stress at the cloud top on the Richardon number has been estimated.

Independent confirmation of the equation of motion should be sought, without which, extrapolation to other cases should be done with caution. However, subject to the qualifications in Sub-section 3.3, it is concluded that the equation of motion is in satisfactory agreement with the data at early and later times for all Phase I trials studied.

References

1 C.J. Wheatley, P.W.M. Brighton and A.J. Prince, Comparison between data from the heavy gas dispersion experiments at Thorney Island and predictions of simple models, In: C. De Wispelaere (Ed.), Proc. 15 th NATO/CCMS Int. Tech. Meeting on Air Pollution Modelling and its Applications, St. Louis, U.S.A., Plenum, New York, 1986, pp. 717–731.

2 C.J. Wheatley, A.J. Prince and P.W.M. Brighton, Comparison between data from the Thorney Island heavy gas trials and predictions of simple dispersion models, UKAEA Report, SRD R 355, Safety and Reliability Directorate, Culcheth, Great Britain, 1986.

3 P.W.M. Brighton, Area-averaged concentrations height-scales and mass balances, J. Hazardous Materials, 11 (1985) 189–208.

4 P.W.M. Brighton, Using concentration data to track clouds in the Thorney Island experiments, UKAEA Report, SRD R 319, Safety and Reliability Directorate, Culcheth, Great Britain, 1986.

5 P.W.M. Brighton, A.J. Prince and D.M. Webber, Determination of cloud area and path from visual and concentration records, J. Hazardous Materials, 11 (1985) 155–178.

6 A.J. Prince, P.W.M. Brighton and D.M. Webber, Thorney Island heavy gas dispersion trials — determination of path and area of cloud from photographs, UKAEA Report, SRD R 318, Safety and Reliability Directorate, Culcheth, Great Britain, 1985.

7 C.I. Bradley, R.J. Carpenter, P.J. Waite, C.G. Ramsay and M.A. English, Recent development of a simple box-type model for dense vapour cloud dispersion, In: S. Hartwig (Ed.), Proc. 2nd Symposium on Heavy Gases and Risk Assessment, Battelle Institute eV, Frankfurt, W. Germany, May 25-26, 1982, D. Reidel, 1982, pp. 77-89.

8 P.C. Chatwin, The dispersion of a puff of passive contaminant in the constant stress region, Q. J. R. Meteorol. Soc., 48 (1968) 345-362.

9 D.G. Beesley, Unpublished SRD memoranda, 1984.

10 D.G. Beesley, Unpublished SRD memoranda, 1985.